Applied and Environmental Microbiology, Mar. 2008, p. 1436–1446 Vol. 74, No. 5
0099-2240/08/$08.00+0 doi:10.1128/AEM.02234-07

NADH Availability Limits Asymmetric Biocatalytic Epoxidation in a Growing Recombinant *Escherichia coli* Strain▽

Bruno Bühler,[1] Jin-Byung Park,[2] Lars M. Blank,[1,3] and Andreas Schmid[1,3]*

Laboratory of Chemical Biotechnology, Dortmund University of Technology, D-44227 Dortmund, Germany[1]; Department of Food Science and Technology, Ewha Womans University, Seoul 120-750, Korea[2]; and Institute for Analytical Sciences, D-44139 Dortmund, Germany[3]

Received 1 October 2007/Accepted 22 December 2007

Styrene can efficiently be oxidized to (*S*)-styrene oxide by recombinant *Escherichia coli* expressing the styrene monooxygenase genes *styAB* from *Pseudomonas* sp. strain VLB120. Targeting microbial physiology during whole-cell redox biocatalysis, we investigated the interdependency of styrene epoxidation, growth, and carbon metabolism on the basis of mass balances obtained from continuous two-liquid-phase cultures. Full induction of *styAB* expression led to growth inhibition, which could be attenuated by reducing expression levels. Operation at subtoxic substrate and product concentrations and variation of the epoxidation rate via the styrene feed concentration allowed a detailed analysis of carbon metabolism and bioconversion kinetics. Fine-tuned *styAB* expression and increasing specific epoxidation rates resulted in decreasing biomass yields, increasing specific rates for glucose uptake and the tricarboxylic acid (TCA) cycle, and finally saturation of the TCA cycle and acetate formation. Interestingly, the biocatalysis-related NAD(P)H consumption was 3.2 to 3.7 times higher than expected from the epoxidation stoichiometry. Possible reasons include uncoupling of styrene epoxidation and NADH oxidation and increased maintenance requirements during redox biocatalysis. At epoxidation rates of above 21 μmol per min per g cells (dry weight), the absence of limitations by O_2 and styrene and stagnating NAD(P)H regeneration rates indicated that NADH availability limited styrene epoxidation. During glucose-limited growth, oxygenase catalysis might induce regulatory stress responses, which attenuate excessive glucose catabolism and thus limit NADH regeneration. Optimizing metabolic and/or regulatory networks for efficient redox biocatalysis instead of growth (yield) is likely to be the key for maintaining high oxygenase activities in recombinant *E. coli*.

Oxygenases catalyze regio- and enantioselective oxyfunctionalization reactions and have a considerable potential in the area of asymmetric organic synthesis (2, 35). These enzymes typically depend on coenzymes such as NAD(P)H and are unstable outside cells, and they often consist of multiple components. Thus, for synthetic applications, their use in whole cells is favored over the use of isolated enzymes (7, 18).

The productivity of oxygenase-based whole-cell biocatalysts is influenced by various factors, such as maximal enzyme activity, enzyme level, substrate mass transfer, substrate and/or product inhibition/toxicity, and cofactor regeneration (7, 13, 54, 68). Enzyme synthesis and cofactor regeneration are related to host metabolism, which in turn may be affected by the toxicity of organic substrates and products. Such toxicity can efficiently be attenuated by regulated substrate feeding (1, 11) and in situ product removal (7, 38, 61, 66, 74). Yet, microbial cells, especially in a nongrowing state, often lose biooxidation activity over time, which may be due to oxygenase inactivation and/or the metabolic burden imposed by redox-coenzyme withdrawal and reactive oxygen species formed via uncoupled oxygen reduction. This led to the use of growing cells as biocatalysts, the metabolism of which supports not only coenzyme regeneration but also continuous oxygenase synthesis and cell reproduction (5, 19, 27, 32, 49). However, during cell growth, various reactions—especially oxidative phosphorylation—consume high amounts of reduction equivalents (59). The synthesis and presence of an active NAD(P)H-consuming oxygenase will thus also influence the metabolism of growing cells; decrease growth yields on energy sources; cause stress; and reduce growth rate, viability, and metabolic activity (4, 9, 58).

Microbial physiology and energy metabolism have been investigated thoroughly for classical fermentation processes but rarely for whole-cell biotransformations (23, 72). In this study, we focus on the interrelation between NADH-dependent styrene epoxidation and central carbon metabolism of growing recombinant *Escherichia coli* (Fig. 1). Thereby, highly active *E. coli* JM101(pSPZ10) (51) expressing the styrene monooxygenase genes *styAB* of *Pseudomonas* sp. strain VLB120 (50) serves as the biocatalyst. The epoxidation activity, growth, and metabolism of *E. coli* JM101(pSPZ10) growing in fed-batch mode in a two-liquid-phase system have been shown to be affected by high styrene oxide concentrations, which caused membrane permeabilization (54). Furthermore, flux balance analysis and in silico and in vivo knockout studies on resting *E. coli* BW25113(pSPZ10) indicated a linear dependency of measured epoxidation activities and simulated NADH regeneration rates of recombinant central carbon metabolism mutants on glucose uptake rates (L. M. Blank, B. E. Ebert, B. Bühler, and A. Schmid, submitted for publication). These results suggested a dependency of the styrene epoxidation efficiency of resting cells on carbon metabolism.

Here, we investigated the interdependency of styrene epoxidation, growth, and carbon metabolism on the basis of mass

* Corresponding author. Mailing address: Laboratory of Chemical Biotechnology, Department of Biochemical and Chemical Engineering, TU Dortmund, Emil-Figge-Str. 66, D-44227 Dortmund, Germany. Phone: 49 231 755 7380. Fax: 49 231 755 7382. E-mail: andreas.schmid@bci.tu-dortmund.de.

▽ Published ahead of print on 11 January 2008.

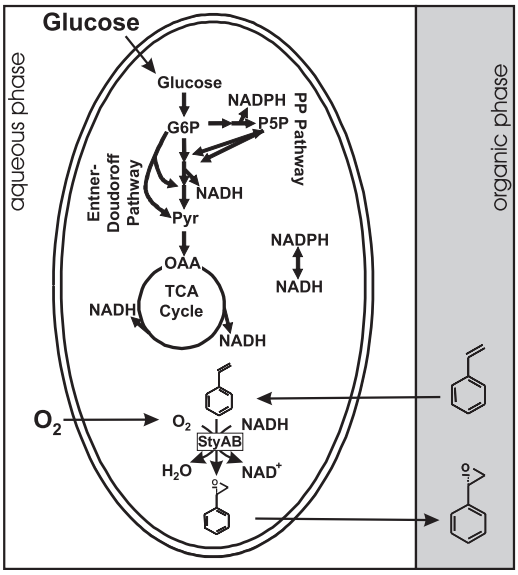

FIG. 1. Schematic of the two-liquid-phase whole-cell styrene epoxidation system. The central carbon metabolism of recombinant *E. coli* fueled with glucose produces biomass precursors, energy, and the reduced redox coenzymes, which serve as electron donors for the epoxidation of styrene catalyzed by the styrene monooxygenase StyAB of *Pseudomonas* sp. strain VLB120. Thereby, molecular oxygen serves as an oxygen donor and the presence of the organic phase minimizes the aqueous concentrations of toxic styrene and styrene oxide. OAA, oxaloacetate; P5P, pentose-5-phosphates..

balances obtained from continuous cultures, allowing for the first time a quantitative insight into the physiology of such biocatalytically active cells. *E. coli* JM101(pSPZ10) was grown at subtoxic substrate and product concentrations in a two-liquid-phase bioreactor system, in which substrate mass transfer over the phase boundary is not limiting (54). Metabolic flux and kinetic analyses were performed using physiological and biotransformation data acquired during steady states with and without induction of *styAB* expression and with various substrate concentrations in the organic-phase feed. Implications of cofactor-dependent oxygenase activity for central carbon metabolism and vice versa are discussed.

MATERIALS AND METHODS

Microorganism and growth media. The organism used in this study was *Escherichia coli* JM101 [*supE thi* Δ(*lac-proAB*) F′(*traD36 lacI*^{q} Δ*lacZM15 proAB*)] (42) harboring plasmid pSPZ10 (51), which contains the styrene monooxygenase genes *styAB* of *Pseudomonas* sp. strain VLB120 (50) under the control of the *alk* regulatory system of *Pseudomonas putida* Gpo1 (40, 65). LB medium containing 1% (wt/vol) glucose and 50 mg liter^{-1} kanamycin was used for the seed culture. Percentages which are not further specified are given as percent weight per volume. For minimal medium precultures, M9* medium, containing three times more phosphate salts than M9 medium (43) but no calcium chloride, was used after supplementation with 5 g liter^{-1} glucose, 50 mg liter^{-1} kanamycin, 10 mg liter^{-1} thiamine, and 1 ml liter^{-1} US* trace element solution as described in detail by Panke et al. (51). MS medium (6) (a modified M9 medium) supplemented as described for the M9* medium was used for controlled growth in bioreactors. During continuous cultivations, the MS medium in the feed tank contained 20 g liter^{-1} glucose.

Continuous cultivation and biotransformation. Experiments were started by batch cultivation in 1 liter MS medium in a stirred tank reactor with a total volume of 3 liters (54, 75). The dissolved oxygen tension (DOT) was determined with an autoclavable amperometric probe (Mettler Toledo, Greifensee, Switzerland), and the pH was automatically kept at 7.1 by feeding 25% NH_4OH. Temperature, aeration rate, and stirrer speed were maintained at 30°C, 2 liters min^{-1}, and 2,000 rpm, respectively. Continuous cultivation was initiated in the late exponential growth phase. In the case of two-liquid-phase cultivations, 0.5 liter of the culture broth was removed and an equal volume of bis(2-ethylhexyl)phthalate (BEHP) (97%; Fluka, Buchs, Switzerland) serving as the organic carrier solvent was added, after steady state had been reached. Aqueous and organic reaction media were supplied at the same rate from two feed tanks. When the system had reached steady state, octane (98%; Acros Organics, Geel, Belgium) or dicyclopropyl ketone (DCPK) (95%; Janssen Chimica, Geel, Belgium), both of which are inducers of the *alk* regulatory system controlling *styAB* expression on plasmid pSPZ10, were added to the culture broth and the feed tank for the organic phase. Inducer concentrations varied and are specified in Results. In order to achieve continuous biotransformation at different rates, various amounts of styrene (99%; Fluka) were added to the organic-phase feed tank and steady states were established. The constituents of the organic phase were used without prior sterilization. Data from independent experiments deviated by a maximum of 10%.

Analytical procedures. Aqueous glucose and acetate concentrations were determined using commercially available kits (TC D-glucose and TC acetic acid; DispoLab, Dielsdorf, Switzerland) after separation of the aqueous phase from the organic phase by centrifugation. Experimental variations amounted to 2.4 and 1.1% for glucose and acetate, respectively. Cell concentrations in the aqueous phase were determined by measuring the optical density at 450 nm as described earlier (10, 54), with an optical density at 450 nm of 1 corresponding to a cell dry weight (CDW) of 0.29 g liter$_{aq}^{-1}$ and an experimental variation of 5.5%.

Styrene, styrene oxide, and 2-phenylethanol concentrations in the organic phase of two-liquid-phase cultivations were determined by gas chromatography after dilution in diethyl ether containing 0.1 mM dodecane as the internal standard and drying over sodium sulfate. For this analysis, we used an Optima 5 column (Macherey-Nagel, Oensingen, Switzerland) connected to a HRGC Mega2 gas chromatograph (Fisons Instruments, Manchester, United Kingdom) with splitless injection and a flame ionization detector. We applied hydrogen as the carrier gas and a temperature profile of 40 to 140°C at 10°C min^{-1} and 140 to 280°C at 20°C min^{-1}. The experimental variations for styrene, styrene oxide, and 2-phenylethanol concentrations in the organic phase amounted to 1.7, 1.9, and 3.6%, respectively.

O_2 and CO_2 contents in the exhaust gas were analyzed with a paramagnetic O_2 analyzer (Servomex oxygen analyzer 540 A; Sybron Taylor, United Kingdom) and an infrared CO_2 analyzer (Binos I; Leubold Heraeus, Germany). The signal was calibrated with pure N_2, normal air, and standard gas. The analytical variations amounted to 1.3 and 5.0% for O_2 and CO_2, respectively. The given experimental and analytical errors for biomass, glucose, acetate, and CO_2 concentrations were used for metabolic flux analysis, which included error propagation.

Resting-cell activity assays. Assays for the determination of specific styrene epoxidation activities were performed as reported previously (50). In short, the assays included harvesting of biomass from an induced culture in M9* medium, resuspension to a defined cell concentration in 0.1 M potassium phosphate buffer (pH 7.4) containing 10 g liter^{-1} glucose, adaptation to reaction conditions, incubation for 5 min with 1.5 mM styrene, extraction with ice-cold diethyl ether containing 0.1 mM dodecane as an internal standard, and determination of substrate and product concentrations by gas chromatography (as described above). Specific reaction rates were calculated based on the amount of (*S*)-styrene oxide formed over time and were expressed as activity per g of CDW [U (g CDW)$^{-1}$]. One unit (U) is defined as the activity that produces 1 μmol of styrene oxide in 1 min.

The kinetics for styrene epoxidation catalyzed by *E. coli* JM101(pSPZ10) in the BEHP-based two-liquid-phase system were estimated by weighted nonlinear regression analysis (Enzfitter; Elsevier-Biosoft, Cambridge, United Kingdom) based on steady-state styrene concentrations and specific activities measured during two-liquid-phase continuous cultivations.

Metabolic flux analysis. The net NAD(P)H regeneration rates were estimated from intracellular flux distributions using a stoichiometric metabolic flux model that comprised glycolysis, the pentose phosphate (PP) pathway, the anaplerotic reaction from phosphoenolpyruvate to oxaloacetate, the tricarboxylic acid (TCA) cycle, and acetate production. Fluxes into biomass were calculated from the known metabolite requirements for macromolecular compounds and the growth rate-dependent RNA and protein contents (16). The stoichiometric matrix of 20 linear equations and 22 metabolites included free interchange between the NADH and NADPH pools by the action of the dissolved and membrane-bound transhydrogenases UdhA and PntAB, respectively (60). This stoichiometric matrix is underdetermined and has a solution space with an infinite number of

different flux vectors that fulfill the constraints derived from the experimentally determined rates for glucose uptake, biomass formation, acetate formation, and CO_2 formation. To uniquely solve the system, an independent linear equation defining the flux ratio between the PP pathway and glycolysis was implemented. We assumed that 55% of glucose-6-phosphate is catabolized through glycolysis as determined by Emmerling et al. (16) for *E. coli* JM101 growing at a dilution rate of 0.09 h^{-1}. Moreover, we assumed phosphoenolpyruvate to oxaloacetate as the only anaplerotic reaction. These two assumptions were considered reasonable because flux ratio variation at the glucose-6-phosphate node and introduction of the glyoxylate shunt as an alternative anaplerotic pathway did not significantly influence the net formation of redox equivalents. Error minimization was carried out as described by Fischer et al. (21). The NADPH pool was balanced, allowing the estimation of a net NADH formation rate. This rate is termed the net NAD(P)H formation rate throughout this paper, as the actual NADH and NADPH formation rates cannot be distinguished by the method applied here. ATP produced via substrate-level phosphorylation was in all cases sufficient to sustain biomass synthesis. Thus, the estimated net amount of NADH formed by glucose catabolism was considered to be directly or indirectly (e.g., via ATP) available for maintenance processes, styrene epoxidation, and other biocatalysis-related processes such as StyAB overproduction, uncoupling, and product extrusion.

RESULTS

Continuous two-liquid-phase cultivation of *E. coli* JM101 (pSPZ10). Styrene oxide has been shown to influence cell growth and carbon metabolism of *E. coli* JM101 by permeabilizing cellular membranes (54). Cell growth was inhibited and acetate formation was promoted in the presence of styrene oxide. Furthermore, *styAB* overexpression resulted in a decrease of growth rates and viability of the host strain. In order to investigate the interrelation between StyAB overproduction, styrene epoxidation, carbon metabolism, and cell growth in more detail, we performed continuous-culture-based biotransformations in a two-liquid-phase system with BEHP as the organic carrier solvent containing subtoxic substrate and product levels.

The dilution rate and the glucose feed concentration were kept constant at 0.1 h^{-1} and 20 g $liter^{-1}$, respectively. The DOT in the culture broth was maintained above 50% to enable high, non-oxygen-limited epoxidation rates and to prevent acetate formation. However, after second-phase addition, the steady-state cell concentration slightly decreased and small amounts of acetate appeared in the medium (results not shown). The presence of the viscous organic phase may have led to incomplete mixing and thus to nonuniform glucose and oxygen concentrations inside the reactor causing acetate formation, as observed in large-scale bioprocesses (17, 25, 46, 62). After the two-liquid-phase culture had attained a steady state, octane was added to the organic phase feed tank (60 mM) and directly into the culture broth to induce *styAB* expression. At the same time ($t = 0$), 80 mM of styrene was added to the organic-phase feed tank (Fig. 2A) (see Materials and Methods for details).

Eight hours after induction, cells sampled during continuous cultivation reached a specific activity of 92 U (g CDW)$^{-1}$ in separate resting-cell activity assays, the same activity as reported for batch- and fed-batch-cultivated cells (54). Fourteen hours after induction, the styrene oxide concentration in the organic phase had increased to 40 mM, leaving only a small amount of styrene in the reaction medium. All input glucose was consumed up to this time point. However, acetate accumulated and the cell concentration started to decrease. In the following period, this decrease accelerated and glucose accumulated in the aqueous phase. This decreasing biocatalyst concentration led to decreasing styrene epoxidation rates and resulted in increasing styrene and decreasing styrene oxide concentrations. In fact, no steady state could be reached during continuous two-liquid-phase biotransformation.

In order to analyze this biotransformation in more detail, we calculated biomass, acetate, and styrene oxide concentrations assuming washout kinetics 22 h after induction (Fig. 2B). Comparison of calculated with experimentally obtained curves indicates cessation of cell growth. However, acetate and in particular styrene oxide concentrations decreased less rapidly than washout would predict. These results show that cell growth becomes completely inhibited during biotransformation with fully induced *E. coli* JM101(pSPZ10) and that cells change metabolism but stay metabolically and biocatalytically active after initiation of styrene epoxidation.

Effect of *styAB* expression on growth of *E. coli* JM101(pSPZ10). In order to elucidate whether growth of *E. coli* JM101(pSPZ10) was inhibited by *styAB* overexpression or styrene epoxidation, we carried out continuous cultivations with various amounts of inducer in the absence of a styrene feed (Fig. 3), profiting from the fact that expression under the control of the *alk* regulatory system can be fine-tuned by controlling the applied inducer concentration (8, 40). For this purpose, we used an aqueous single-phase medium instead of an organic/aqueous emulsion. DCPK instead of octane was used for induction, as this inducer allows a better control of gene expression due to its lower volatility and the higher inducer concentration levels required for full induction (8).

When *E. coli* JM101(pSPZ10) was fully induced with 4.2 mM DCPK, cells sampled during continuous cultivation reached a specific activity of 94 U (g CDW)$^{-1}$ in whole-cell assays. This resulted in a strong inhibition of cell growth and washout (Fig. 3) in a very similar manner as seen in the continuous biotransformation shown in Fig. 2. In contrast, a DCPK concentration of 0.17 mM in the aqueous medium, leading to a specific activity of 52 U (g CDW)$^{-1}$ in resting-cell assays, resulted in steady-state growth of *E. coli* JM101(pSPZ10) and in a slight reduction of the biomass yield. The octane and DCPK concentrations applied here did not have a significant influence on growth of *E. coli* JM101 in batch cultures (8). Thus, the severe growth inhibition during the continuous biotransformation shown in Fig. 2 can be attributed to high-level *styAB* overexpression, an effect also observed for alkane monooxygenase-overproducing *E. coli* (20). In the case of *E. coli* JM101(pSPZ10), such severe growth inhibition can be avoided by reducing the induction level via fine-tuning of the inducer concentration.

Continuous styrene biotransformation at various rates. On the basis of the results achieved with a reduced *styAB* expression level, we were then able to investigate the interrelation between styrene epoxidation and carbon and energy metabolism of *E. coli* JM101(pSPZ10) in the two-liquid-phase system. We performed continuous-cultivation-based biotransformations under the same conditions as in the experiment shown in Fig. 2 except for the inducer of *styAB* expression, which was DCPK instead of octane.

In the two-liquid-phase system, a DCPK concentration of 1.7 mM in the organic phase was found to induce the cells to a specific activity of 50 U (g CDW)$^{-1}$ as determined in separate

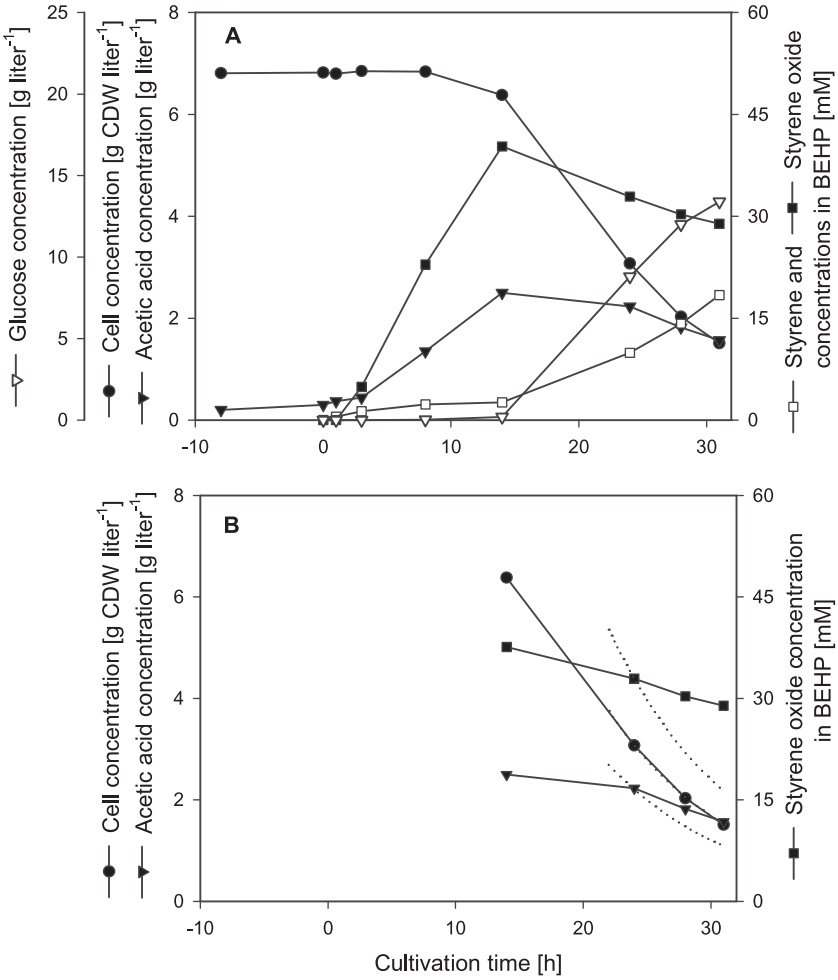

FIG. 2. Continuous biotransformation with fully induced *E. coli* JM101(pSPZ10) in a two-liquid-phase system. BEHP was used as the organic carrier solvent at a phase ratio of 1:1 in a 1-liter working volume. The dilution rates for the organic and aqueous phases were set at 0.1 h^{-1}. Styrene epoxidation was initiated at $t = 0$ by adding 60 mM of the inducer octane into the reactor and the organic-phase feed tank and 80 mM of styrene into the organic-phase feed tank. See Materials and Methods for further details. (A) Courses of biomass, glucose, and acetate concentrations in the aqueous phase and of styrene and styrene oxide concentrations in the organic phase. (B) Solid lines, experimental data; dotted lines, calculated wash-out kinetics after $t = 22$ h. Results were confirmed by an independent experiment.

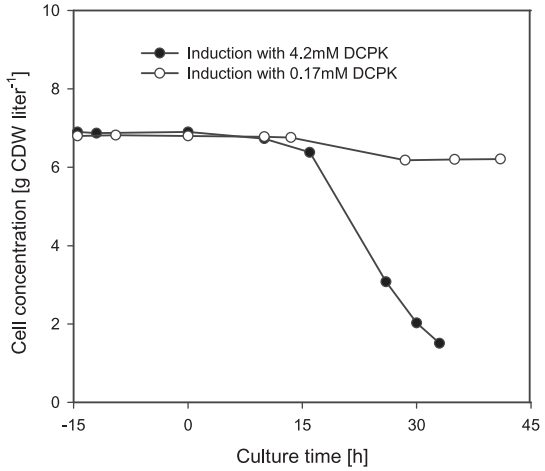

FIG. 3. Expression of *styAB* to different activity levels during continuous cultivation ($D = 0.1$ h^{-1}) of *E. coli* JM101(pSPZ10) in an aqueous single-phase system. The cells were induced at $t = 0$ by adding 4.2 or 0.17 mM of DCPK into the reactor and the feed tank. See Materials and Methods for details.

whole-cell activity assays with cells sampled during steady-state growth. Induction of *styAB* expression to this activity caused the cell concentration in the aqueous phase to decrease from 6.4 to 6.1 g CDW liter^{-1}, as shown by the switch from steady-state I to steady-state II in the continuous biotransformation shown in Fig. 4. In parallel, the O_2 uptake and CO_2 evolution rates increased from 3.9 to 4.4 and from 5.6 to 6.2 mmol (g CDW)$^{-1}$ h^{-1}, respectively (Fig. 4A). The decrease in biomass yield and the concomitant increase of O_2 uptake and CO_2 evolution rates under carbon-limited conditions indicate that *styAB* expression increases the energy requirements of the cells.

In order to investigate styrene epoxidation at different rates and its effect on growth and metabolism, the styrene concentration in the organic feed was increased stepwise from 0 to 131 mM (Fig. 4C). This enabled the establishment of a set of different steady states (steady-states III to VI in Fig. 4 and Table 1), in which we observed a stepwise increase of the styrene and styrene oxide concentrations in the organic phase

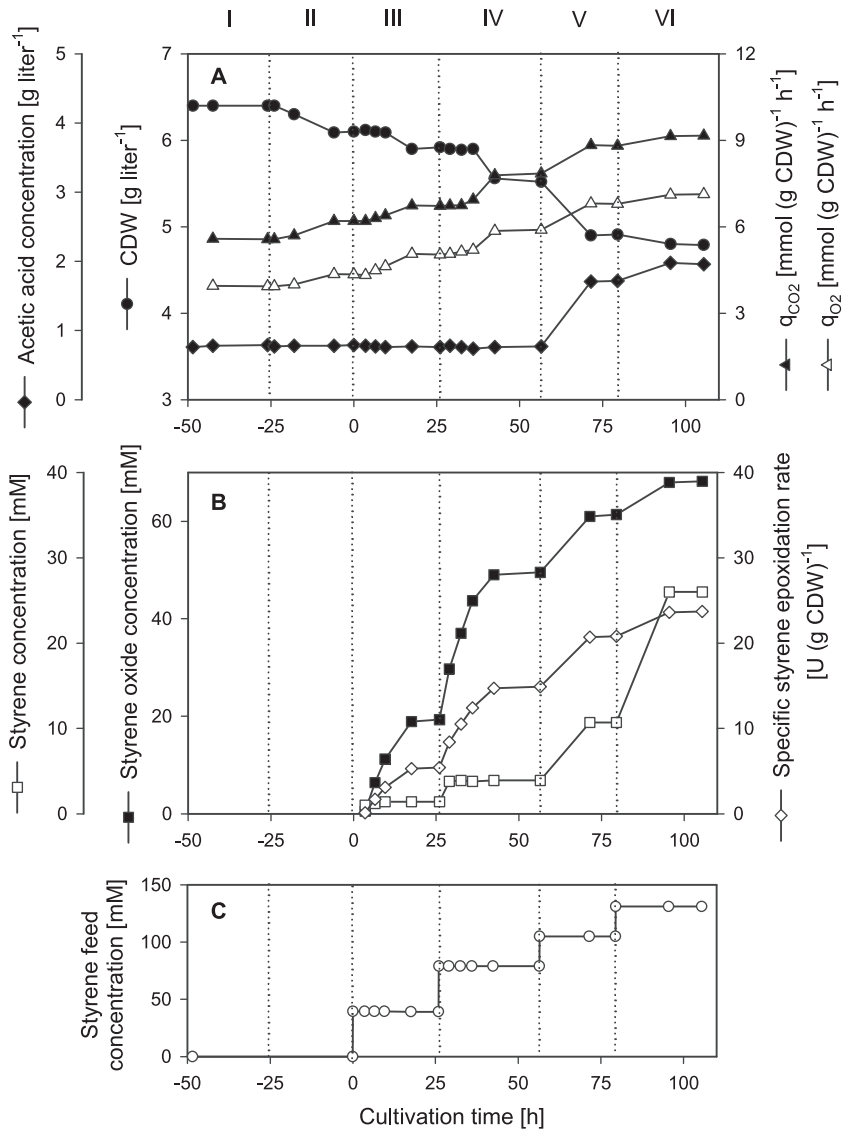

FIG. 4. Fine-tuned induction of *E. coli* JM101(pSPZ10) and styrene epoxidation at various rates during continuous two-liquid-phase cultivation ($D = 0.1\ h^{-1}$). At $t = -25$ h, *styAB* expression was induced with an organic DCPK concentration of 1.7 mM. Styrene epoxidation was initiated at $t = 0$ by adding 40 mM styrene into the organic-phase feed tank. The other conditions were the same as in the experiment shown in Fig. 2. The results obtained during steady-states I to III were confirmed by an independent experiment, in which data deviated by at maximum 10% from those in the experiment shown. (A) Courses of biomass and acetate concentrations in the aqueous phase and of the specific O_2 uptake rate (q_{O2}) and the specific CO_2 evolution rate (q_{CO2}). (B) Styrene and styrene oxide concentrations in the organic phase and specific styrene epoxidation rates. (C) Styrene feed concentrations applied.

and thus of the styrene epoxidation rate, confirming styrene limitation. With a styrene feed concentration of 131 mM (steady-state VI), styrene oxide accumulated to 68 mM in the organic phase at specific and volumetric activities of 24 U (g CDW)$^{-1}$ and 110 U per liter aqueous phase, respectively (Fig. 4B; Table 1). During this steady state, 52% of the input styrene had been transformed to styrene oxide; 5% was converted into 2-phenylethanol, a by-product of styrene epoxidation (51, 54); and 23% was considered to be lost by evaporation. However, the specific activity reached in steady-state VI was only half of the maximal activity reached in resting-cell assays. This, the fact that oxygen was not limiting during continuous cultivation and biotransformation (DOT of >50%), and the small increase of the specific epoxidation rate during the switch from steady-state V to VI, when the styrene concentration in the organic phase steeply increased from 11 to 26 mM (Fig. 4B), indicate that NADH and not styrene or O_2 was the substrate limiting the epoxidation rate in steady-state VI.

In parallel to the stepwise increase of the epoxidation rate, the cell density decreased stepwise, accompanied by a stepwise increase of the specific O_2 uptake and CO_2 evolution rates (Fig. 4B). The acetate concentration increased markedly when the styrene conversion rate exceeded 15 U (g CDW)$^{-1}$ (steady-states V and VI in Fig. 4 and Table 1). These results show that cell growth and carbon metabolism are both influenced by styrene epoxidation.

TABLE 1. Growth and biotransformation parameters during continuous cultivation of *E. coli* JM101(pSPZ10)[a]

Steady state[b]	Styrene feed concn (mM)	Cell concn (g CDW $liter_{aq}^{-1}$)	Styrene oxide concn (mM)[c]	Styrene concn (mM)[c]	Specific epoxidation rate [U (g CDW)$^{-1}$]	Acetate concn (g $liter_{aq}^{-1}$)	Carbon balance (%)			
							Biomass	Acetate	CO_2	Sum
I	0	6.4				0.78	38	4	54	97
II[d]	0	6.1				0.78	36	4	57	97
III	39	5.9	19	1.4	5	0.76	35	4	60	99
IV	79	5.5	49	3.9	15	0.76	33	4	65	102
V	105	4.9	61	11	21	1.72	29	9	65	103
VI	131	4.8	68	26	24	1.97	28	10	66	104

[a] The dilution rates for the organic and aqueous phases were set at 0.1 h^{-1}. See Materials and Methods for details. The standard deviations of duplicate measurements were below 5%. aq, aqueous phase.
[b] The steady states refer to the experiment shown in Fig. 4.
[c] Concentrations in the organic phase are given.
[d] Steady-state II was established by adding the inducer DCPK to the bioreactor and the feed tank to a concentration of 1.7 mM in the organic phase.

Metabolic flux analysis during biotransformation. During styrene epoxidation with growing *E. coli* JM101(pSPZ10), glucose is used for biomass synthesis, including the synthesis of heterologous StyAB; for energy [NAD(P)H and ATP] generation, which leads to O_2 consumption and CO_2 formation; and for the regeneration of the NADH required for styrene epoxidation. Additional energy may be required for associated reactions such as uncoupling and 2-phenylethanol formation and for sustaining the presence of heterologous StyAB and toxic compounds. Moreover, the carbon source can be channeled into acetate when the carbon flux into the central metabolic pathways exceeds the activity of the TCA cycle during aerobic growth on glucose (56, 70, 71).

The carbon balances (Table 1) for the different steady states during the continuous cultivation shown in Fig. 4 reveal that an increase of the epoxidation rate resulted in a decrease of the biomass yield and an increase of the fraction of glucose converted into CO_2 (steady-states I to IV) and acetate (steady-states V and VI). In order to investigate carbon and energy metabolism during styrene epoxidation in more detail, we performed metabolic flux analysis based on the data shown in Table 1 and on a stoichiometric model for the central carbon metabolism of *E. coli* (see Materials and Methods). As shown in Fig. 5, induction and increasing epoxidation rates led to increasing specific glucose uptake rates and influenced the flux distribution through central carbon metabolism. Induction and biocatalysis up to specific epoxidation rates of 15 U (g CDW)$^{-1}$ (steady-states I to IV) resulted in increased relative fluxes through the TCA cycle. A further increase of the specific epoxidation rate to 21 U (g CDW)$^{-1}$ (steady-state V) led to a stagnating relative but still increasing absolute TCA cycle flux and to significantly enhanced acetate formation. A further

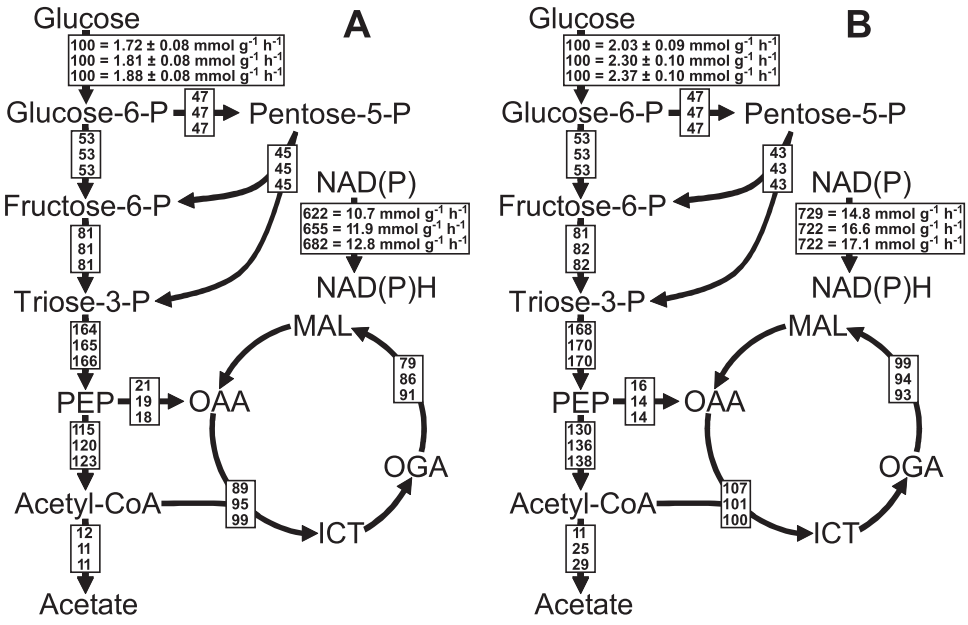

FIG. 5. Relative distributions of absolute carbon fluxes in *E. coli* central carbon metabolism during steady-states I to III (A, top to bottom) and IV to VI (B, top to bottom) of the experiment shown in Fig. 4. All fluxes are normalized to the specific glucose uptake rates, which correspond to the absolute fluxes given for glucose phosphorylation. Absolute fluxes are also given for the net NAD(P)H formation rate, which corresponds to the total NAD(P)H formation by glucose catabolism minus the amount of NAD(P)H consumed for net biomass synthesis. The contribution of the PP pathway toward glucose-6-phosphate (glucose-6-P) consumption was set to 45% (16). PEP, phosphoenolpyruvate; CoA, coenzyme A; OAA, oxaloacetate; MAL, malate; OGA, 2-oxoglutarate; ICT, isocitrate.

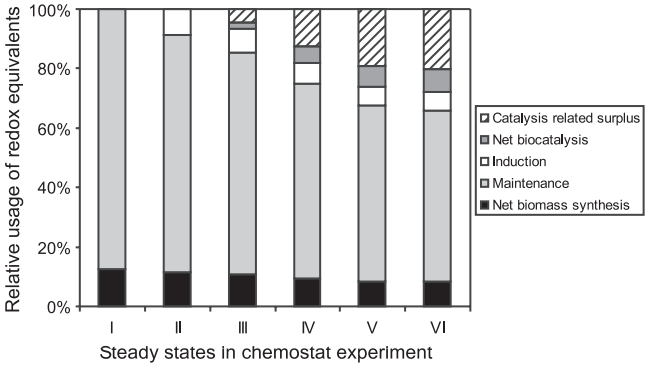

FIG. 6. Relative usage of the redox equivalents [NAD(P)H] produced by glucose catabolism during the continuous cultivation shown in Fig. 4. In the absence of induction and biotransformation in steady-state I, NAD(P)H is consumed for net biomass synthesis and maintenance requirements (e.g., transport processes and macromolecule turnover), which were assumed to remain constant during induction and biotransformation. Under biotransformation conditions, the total amount of NAD(P)H formed is further subdivided into redox equivalents consumed for *styAB* expression (induction, constant requirements were assumed), NADH consumed for net biocatalysis with a stoichiometry of 1 mol per mol styrene oxide produced, and surplus redox equivalents consumed during biocatalysis.

increase of the styrene concentration, however, resulted in minor increases of glucose uptake, TCA cycle, and acetate formation rates, which corresponds to the minor increase of the specific epoxidation rate (steady-state VI). In total, the specific net NAD(P)H formation rate, corresponding to the total NAD(P)H formation rate during glucose catabolism minus the rate at which NAD(P)H is consumed for net biomass synthesis, increased by 65%, comparing steady-states I and VI (Fig. 5). This and the reduced biomass yield on glucose reveal that styrene epoxidation results in a clearly higher NAD(P)H demand in recombinant *E. coli*.

To determine what the consumed NAD(P)H was used for in biocatalytically active *E. coli*, we estimated, on the basis of the stoichiometric model and the biotransformation data, the relative amount of NAD(P)H utilized for net biomass synthesis, maintenance requirements, *styAB* expression, and styrene epoxidation during the different steady states (Fig. 6). Assuming a constant NAD(P)H demand for growth, maintenance, and StyAB synthesis during styrene epoxidation, the biocatalysis-related consumption of reduced redox equivalents could be calculated. Surprisingly, the biocatalysis-related NAD(P)H consumption exceeded the stoichiometric NADH demand for styrene epoxidation by a factor of 3.2 to 3.7. Possible causes for this surplus demand for reduced nicotinamide coenzymes include increased maintenance requirements during biocatalysis or StyAB-related processes such as by-product formation and uncoupling, as discussed below.

In general, we conclude that styrene epoxidation at increasing rates led to saturation of the TCA cycle and acetate formation, indicating a biological energy shortage, which may well be responsible for the limitation of the styrene epoxidation rate in steady-state VI.

DISCUSSION

Reported productivities of oxygenase-based whole-cell biocatalysts have reached levels suitable for industrial implementation (7, 53, 67). Yet, only a few such processes have been scaled to production level, since biotransformation rates typically are rather unstable and activities during long-term biotransformations are often lower than maximal activities obtained in short-term assays with whole cells (6, 10, 48, 54), cell extracts (13), and enriched enzyme preparations (26). The physiology of whole-cell redox biocatalysts during long-term biotransformations is largely unknown, although it is influenced by biocatalysis and may at least in part be responsible for limited biocatalyst activities and stabilities. During continuous cultivation, we observed that *styAB* overexpression had negative long-term effects on the growth and metabolism of *E. coli* JM101(pSPZ10) and its biocatalytic activity (Fig. 1 and 2). Compromised viability and membrane functionality has been observed earlier for xylene monooxygenase- and StyAB-producing recombinant *E. coli* JM101 (37, 54). Here, by reducing the inducer concentration, we were able to achieve stable StyAB activities during continuous cultivation. Furthermore, a BEHP-based two-liquid-phase system allowed operation of the biocatalyst at subtoxic, noninhibitory product levels and enabled efficient substrate mass transfer and uptake by recombinant *E. coli* (54). Increasing the styrene concentration and thus the steady-state epoxidation rate in this system allowed us to investigate whether NADH availability and thus the microbial energy metabolism limit styrene epoxidation above a certain rate.

Effect of NADH availability on styrene epoxidation. Metabolic flux analysis showed that increasing epoxidation rates led to increasing fluxes through and saturation of the TCA cycle and to acetate formation. This, the absence of oxygen limitation, and the fact that the small increase of the specific epoxidation rate during the switch from steady-state V to VI did not correlate with the steep increase of the styrene concentration (Fig. 4B) indicated that NADH becomes limiting at increasing epoxidation rates. This finding is supported by the correlation of the relatively small increases of specific epoxidation and NAD(P)H formation rates between steady-states V and VI (Fig. 5).

In order to further investigate the kinetics of styrene epoxidation during continuous cultivation, we performed weighted nonlinear regression analyses on the basis of Michaelis-Menten kinetics. Thereby, specific epoxidation rates measured during steady-states III to VI of the continuous cultivation shown in Fig. 4 and of an independent steady state were related directly to the styrene concentrations in the organic phase without considering phase transfer (Fig. 7). This is reasonable, as mass transfer over the phase boundary has been shown not to be limiting in the system under investigation and recombinant *E. coli* strains have been found to take up aromatic hydrocarbons such as styrene and pseudocumene directly from the organic phase (9, 54). Such direct styrene uptake also becomes obvious considering the kinetics given by the curve in Fig. 7 based on the K_s (64 ± 14 μM) for the aqueous single-phase system (54), aqueous styrene concentrations calculated via the partition coefficient for styrene (2,990 ± 200) (54), and a V_{max} of 50 U (g CDW)$^{-1}$ as determined in activity assays after reduced

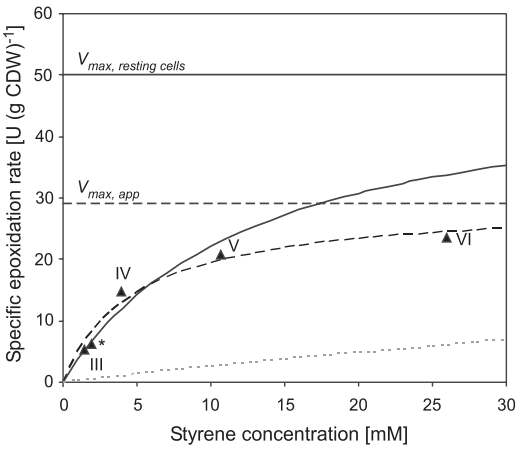

FIG. 7. Michaelis-Menten plot of styrene concentrations in the organic phase and specific epoxidation rates measured during steady-states III to VI of continuous two-liquid-phase cultivation (Table 1; Fig. 4). A data point from an independent steady state is indicated by a star. The dotted curve shows the rates calculated via the K_s (64 ± 14 μM) for the aqueous single-phase system (54), aqueous styrene concentrations derived from the partition coefficient for styrene (2,990 ± 200) (54), and a V_{max} of 50 U (g CDW)$^{-1}$ as determined in activity assays after reduced induction. The dashed curve represents a weighted nonlinear regression based on data from steady-states III to VI and *, giving a K_s of 4.9 ± 1.3 mM and an apparent V_{max} of 29.0 ± 2.7 U (g CDW)$^{-1}$ (indicated as $V_{max,app}$). The solid curve represents a weighted nonlinear regression based on data from steady-states III to V, as well as steady-state *, and on a V_{max} of 50 U (g CDW)$^{-1}$ as determined in separate resting-cell activity assays (indicated as $V_{max,resting\ cells}$). The estimated K_s is 12.7 ± 1.9 mM.

induction. The specific activities during continuous two-liquid-phase cultivation indeed followed Michaelis-Menten kinetics (Fig. 7) as found during continuous cultivation of styrene oxide isomerase-deficient *Pseudomonas* sp. strain VLB120ΔC in the same two-liquid-phase system. The apparent K_s value obtained (4.9 ± 1.3 mM), however, was significantly lower than the 18.8 ± 1.3 mM for *Pseudomonas* sp. strain VLB120ΔC (55). Furthermore, the V_{max} obtained for the *Pseudomonas* mutant perfectly matched the maximal specific activity derived from resting-cell assays (55), whereas recombinant *E. coli* showed an apparent V_{max} of 29.0 ± 2.7 U (g CDW)$^{-1}$, which is significantly below the 50 U (g CDW)$^{-1}$ determined in activity assays. This discrepancy indicates that the fit to styrene-dependent Michaelis-Menten kinetics is misleading and that, at increasing rates, styrene epoxidation indeed becomes limited by the NADH availability in growing *E. coli* JM101(pSPZ10). In order to evaluate whether NADH limitation was especially significant at high styrene concentrations, we excluded steady-state VI but included a V_{max} of 50 U (g CDW)$^{-1}$ in the weighted nonlinear regression analysis. This as well allowed a reasonable fit to Michaelis-Menten kinetics, with a K_s of 12.7 ± 1.9 mM (Fig. 7), confirming that styrene epoxidation during steady-state VI was limited mainly by NADH and not by styrene.

It is clear that, depending on the reaction conditions (induction level, glucose and oxygen availability, growth rate, and substrate and product concentrations), the NADH flux distribution to the different NADH-dependent reactions and thus the achievable specific epoxidation rate may vary considerably. This explains why substantially higher epoxidation rates of up to 60 U (g CDW)$^{-1}$ have been achieved during fed-batch cultivation of *E. coli* JM101(pSPZ10) (49, 51, 52).

Possible causes for the surplus NAD(P)H demand during styrene epoxidation. As shown in Fig. 6, the biocatalysis-related NAD(P)H consumption exceeded the stoichiometric NADH demand for styrene epoxidation by a factor of 3.2 to 3.7. This surplus demand for reduced nicotinamide coenzymes, which obviously correlates with the specific epoxidation rate, may be caused by increased maintenance requirements during biocatalysis and/or StyAB-related effects such as by-product formation and uncoupling.

During styrene epoxidation, 2-phenylethanol is formed as a by-product. This by-product formation consumes 2 mol of NADH per mol styrene converted and thus represents an additional NADH sink (54). The 2-phenylethanol formation rate amounted to about 7% of the styrene oxide formation rate and thus increased the NADH demand by 14%. This, however, explains only a small fraction of the surplus NAD(P)H demand. Uncoupling might contribute more significantly to high coenzyme consumption rates. Styrene monooxygenase is a two-component flavoenzyme composed of the NADH-specific flavin reductase StyB and the reduced flavin adenine dinucleotide ($FADH_2$)-dependent styrene epoxidase StyA, with freely diffusible FAD(H_2) serving as the electron shuttle between the two subunits (47). Instead of activating molecular oxygen for oxygenation reactions, $FADH_2$ can be reoxidized in two different types of uncoupling reactions. It reacts either with molecular oxygen to yield hydrogen peroxide and FAD or with FAD to form highly reactive flavin radicals, which can react with molecular oxygen to form hydrogen peroxide (41). In vitro, uncoupling accounted for up to 80% of the NADH consumption and depended on the FAD concentration and the StyA/StyB ratio (30, 47). The extent of uncoupling under in vivo conditions is not known so far. However, beside the metabolic burden of recombinant gene expression in *E. coli* (3, 14, 24, 63), uncoupling might partly be responsible for the increased NAD(P)H demand of induced cells in the absence of styrene in steady-state II and substantially contribute to the high biocatalysis-related NAD(P)H consumption observed during styrene epoxidation in steady-states III to VI (Fig. 6). In the latter case, a substrate-induced type of uncoupling would best explain the correlation between epoxidation and NAD(P)H consumption rates.

A biocatalysis-related increase of maintenance requirements is another possible reason for the high NAD(P)H consumption during styrene epoxidation. Above a certain concentration, small apolar compounds such as styrene, styrene oxide, and 2-phenylethanol are toxic to living cells owing to various effects, of which membrane disintegration is believed to be the most prominent (34, 64). Such lipophilic substances accumulate in the cellular membrane bilayer and finally result in membrane permeabilization and cell lysis. Since membrane permeabilization impairs the function of the membranes as a matrix for embedded proteins and as a selective barrier, metabolic activity of cells, which is critical for cofactor regeneration and protein synthesis, can be influenced by organic chemicals. According to the toxicity data for styrene and its products (54), these compounds were present at subtoxic concentrations during the continuous biotransformation experiments performed

in this study. In the absence of styrene epoxidation, styrene oxide, for example, had no influence on cell growth and acetate formation at concentrations of below 150 mM in the organic phase (54). During biotransformation, however, products are formed inside the cells, which may lead to toxic effects at substantially lower detectable product concentrations. This would cause increased NAD(P)H and ATP demands for active solvent extrusion and compensation of proton gradient dissipation. Such increased maintenance demands would increase with increasing product formation rates as observed during continuous cultivation (Fig. 4 and 6).

Interestingly, styrene oxide isomerase-deficient *Pseudomonas* sp. strain VLB120ΔC showed higher styrene oxide and biomass yields on glucose than did *E. coli* JM101(pSPZ10) and did not show any by-product formation (55), indicating a more efficient coupling of styrene epoxidation to biocatalysis-related NADH consumption.

Carbon metabolism of recombinant *E. coli* during styrene epoxidation. During continuous two-liquid-phase cultivation at a constant dilution rate, *styAB* expression and styrene epoxidation at increasing turnover rates caused increases in the specific rates of glucose uptake (38%), the TCA cycle (69%), and net NAD(P)H formation (65%, not considering the amount used for net biomass synthesis [Fig. 5]). Similarly, Vemuri et al. observed increased specific glucose uptake as well as CO_2 and thus NAD(P)H formation rates and decreased biomass yields when an active NADH oxidase catalyzing the reduction of O_2 to H_2O was present in recombinant *E. coli* MG1655 (71). However, during glucose-limited growth, this strain showed reduced acetate formation, whereas *E. coli* JM101(pSPZ10) showed increasing acetate formation at styrene epoxidation rates of above 15 U (g CDW)$^{-1}$ (Fig. 4 and 5). Typically, wild-type *E. coli* strains, including *E. coli* JM101, form acetate above critical glucose uptake rates of 3.4 to 5.5 mmol (g CDW)$^{-1}$ h^{-1} at growth rates and temperatures of between 0.35 and 0.4 h^{-1} and 28 and 37°C, respectively (16, 31, 44). The presence of NADH oxidase increased the critical glucose uptake rate from 4.44 to 6.67 mmol (g CDW)$^{-1}$ h^{-1} at growth rates of between 0.40 and 0.36 h^{-1} (71), whereas styrene epoxidation caused pronounced acetate formation already at glucose uptake rates of above 2 mmol (g CDW)$^{-1}$ h^{-1} and a low growth rate of 0.1 h^{-1}.

Interestingly, Vemuri et al. found that knockout of ArcA, a component of the ArcB/ArcA signal transduction system regulating gene expression in response to redox conditions (22, 36, 39), also led to an increase of the critical glucose uptake rate (71) and that the cumulative effect of NADH oxidase expression and *arcA* knockout can be used to improve recombinant protein production, which often is acetate sensitive (73). The reduced acetate formation at high glucose uptake rates in NADH oxidase-containing *E. coli* correlated with a reduction of the NADH/NAD ratio, which was proposed to contribute to the regulation of the TCA cycle and acetate formation (71). During styrene epoxidation, however, the high biocatalysis-related NADH consumption rate did not prevent acetate formation. Furthermore, a plateau in the specific oxygen uptake rate, which typically is observed at the onset of acetate formation and constitutes the maximal respiration capacity (15, 69), was not reached during styrene epoxidation. The oxygen uptake rate in steady-state VI [7.13 mmol (g CDW)$^{-1}$ h^{-1}], also including the StyAB-related oxygen consumption, was far lower than the maximal rate determined, e.g., for *E. coli* W3110 [15 mmol (g CDW)$^{-1}$ h^{-1}] (69). Thus, a different level of regulation seems to be responsible for acetate formation during oxygenase catalysis, which also was observed in earlier studies (6, 54).

A main difference between NADH oxidase and StyAB catalysis consists of the type of products involved. Whereas water produced from molecular oxygen is not expected to affect cell physiology, styrene oxide and 2-phenylethanol both are toxic and affect membrane integrity and functionality as well as viability (37, 54). Stress imposed by these products as well as by oxygenase overexpression (34) might in fact have caused the observed early saturation of the TCA cycle, acetate formation, and stagnating glucose uptake rates. Elevated acetate formation and uncoupling of StyAB catalysis leading to the formation of reactive oxygen species might have contributed to this stress. In fact, proteomic analyses via two-dimensional electrophoresis and mass spectrometry revealed a strong increase in the level of PspA, a major effector of the phage shock protein (Psp) response (12, 29), during styrene epoxidation in two-liquid-phase fed-batch cultures (A. Schmid et al., unpublished results). The Psp response is induced by a variety of membrane-altering stresses, including exposure to hydrophobic solvents (33), and was proposed to play a role in maintaining cytoplasmic membrane integrity and adjusting energy metabolism and proton motive force by, e.g., promoting anaerobic respiration and fermentation (12, 29). Interestingly, ArcB is involved in the induction of the Psp response, which on the other hand seems to activate the ArcB/ArcA modulon (29). This activation of the ArcB/ArcA modulon by the Psp stress response might be responsible for repression of the TCA cycle and acetate formation during styrene epoxidation and might thus even promote NADH limitation. This is reasonable as, in the absence of the Psp stress response, ArcA was shown to regulate TCA cycle activity in an ArcB-independent way under both aerobic and anaerobic conditions (56), a mechanism, which might depend more directly on the NADH/NAD ratio. As ArcA also represses *ptsG* expression (28), Psp/ArcB/ArcA-dependent regulation may be responsible for the saturation-type behavior not only of the TCA cycle but also of glucose uptake (Fig. 5) and might explain the differences observed between NADH oxidase- and StyAB-containing *E. coli* strains. Such control of the energy metabolism of biocatalytically active *E. coli*, which may involve further global regulators, may prevent energy dissipation and wastage of the limiting carbon and energy source and thus preserve a certain biomass yield during energy-limited growth under stress conditions. This can also be considered as a trade-off between rate and yield, as was proposed from an evolutionary point of view (45, 57).

From an application point of view, control of physiological stress either via efficient in situ removal of toxic products or by redirecting carbon and energy metabolism during biotransformation is likely to be the key for maintaining high catalytic activity of recombinant *E. coli* in biooxidations. In general, it will be of great interest to investigate the productivity-determining interactions between carbon and energy metabolism during redox biocatalysis in more detail.

ACKNOWLEDGMENTS

We thank Bernard Witholt for valuable and inspiring discussions and for providing laboratory facilities.

The financial support from the Deutsche Bundesstiftung Umwelt (DBU), the European Union (EFRE), and the Ministry of Innovation, Science, Research and Technology of North Rhine-Westphalia is gratefully acknowledged.

REFERENCES

1. **Amanullah, A., C. J. Hewitt, A. W. Nienow, C. Lee, M. Chartrain, B. C. Buckland, S. W. Drew, and J. M. Woodley.** 2002. Fed-batch bioconversion of indene to cis-indandiol. Enzyme Microb. Technol. **31:**954–967.
2. **Besse, P., and H. Veschambre.** 1994. Chemical and biological synthesis of chiral epoxides. Tetrahedron **50:**8885–8927.
3. **Bhattacharya, S. K., and A. K. Dubey.** 1995. Metabolic burden as reflected by maintenance coefficient of recombinant *Escherichia coli* overexpressing target gene. Biotechnol. Lett. **17:**1155–1160.

3a. **Blank, L. M., B. E. Ebert, B. Bühler, and A. Schmid.** Metabolic capacity estimation of *Escherichia coli* as platform for redox biocatalysis. Constraint based modeling and experimental verification. Biotechnol. Bioeng., in press.

4. **Bosetti, A., J. B. van Beilen, H. Preusting, R. G. Lageveen, and B. Witholt.** 1992. Production of primary aliphatic alcohols with a recombinant *Pseudomonas* strain, encoding the alkane hydroxylase system. Enzyme Microb. Technol. **14:**702–708.
5. **Bühler, B., I. Bollhalder, B. Hauer, B. Witholt, and A. Schmid.** 2003. Chemical biotechnology for the specific oxyfunctionalization of hydrocarbons on a technical scale. Biotechnol. Bioeng. **82:**833–842.
6. **Bühler, B., I. Bollhalder, B. Hauer, B. Witholt, and A. Schmid.** 2003. Use of the two-liquid phase concept to exploit kinetically controlled multistep biocatalysis. Biotechnol. Bioeng. **81:**683–694.
7. **Bühler, B., and A. Schmid.** 2004. Process implementation aspects for biocatalytic hydrocarbon oxyfunctionalization. J. Biotechnol. **113:**183–210.
8. **Bühler, B., A. Schmid, B. Hauer, and B. Witholt.** 2000. Xylene monooxygenase catalyzes the multistep oxygenation of toluene and pseudocumene to corresponding alcohols, aldehydes, and acids in *Escherichia coli* JM101. J. Biol. Chem. **275:**10085–10092.
9. **Bühler, B., A. J. J. Straathof, B. Witholt, and A. Schmid.** 2006. Analysis of two-liquid-phase multistep biooxidation based on a process model: indications for biological energy shortage. Org. Proc. Res. Dev. **10:**628–643.
10. **Bühler, B., B. Witholt, B. Hauer, and A. Schmid.** 2002. Characterization and application of xylene monooxygenase for multistep biocatalysis. Appl. Environ. Microbiol. **68:**560–568.
11. **Carragher, J. M., W. S. McClean, J. M. Woodley, and C. J. Hack.** 2001. The use of oxygen uptake rate measurements to control the supply of toxic substrate: toluene hydroxylation by *Pseudomonas putida* UV4. Enzyme Microb. Technol. **28:**183–188.
12. **Darwin, A. J.** 2005. The phage-shock-protein response. Mol. Microbiol. **57:**621–628.
13. **Doig, S. D., H. Simpson, V. Alphand, R. Furstoss, and J. M. Woodley.** 2003. Characterization of a recombinant *Escherichia coli* TOP10 [pQR239] whole-cell biocatalyst for stereoselective Baeyer-Villiger oxidations. Enzyme Microb. Technol. **32:**347–355.
14. **Dong, H. J., L. Nilsson, and C. G. Kurland.** 1995. Gratuitous overexpression of genes in *Escherichia coli* leads to growth inhibition and ribosome destruction. J. Bacteriol. **177:**1497–1504.
15. **Eiteman, M. A., and E. Altman.** 2006. Overcoming acetate in *Escherichia coli* recombinant protein fermentations. Trends Biotechnol. **24:**530–536.
16. **Emmerling, M., M. Dauner, A. Ponti, J. Fiaux, M. Hochuli, T. Szyperski, K. Wüthrich, J. E. Bailey, and U. Sauer.** 2002. Metabolic flux responses to pyruvate kinase knockout in *Escherichia coli*. J. Bacteriol. **184:**152–164.
17. **Enfors, S. O., M. Jahic, A. Rozkov, B. Xu, M. Hecker, B. Jurgen, E. Kruger, T. Schweder, G. Hamer, D. O'Beirne, N. Noisommit-Rizzi, M. Reuss, L. Boone, C. Hewitt, C. McFarlane, A. Nienow, T. Kovacs, C. Tragardh, L. Fuchs, J. Revstedt, P. C. Friberg, B. Hjertager, G. Blomsten, H. Skogman, S. Hjort, F. Hoeks, H. Y. Lin, P. Neubauer, R. van der Lans, K. Luyben, P. Vrabel, and A. Manelius.** 2001. Physiological responses to mixing in large scale bioreactors. J. Biotechnol. **85:**175–185.
18. **Faber, K.** 2004. Biotransformations in organic chemistry, 5th ed. Springer, Berlin, Germany.
19. **Favre-Bulle, O., E. Weenink, T. Vos, H. Preusting, and B. Witholt.** 1993. Continuous bioconversion of *n*-octane to octanoic acid by recombinant *Escherichia coli* (*alk*$^+$) growing in a two-liquid-phase chemostat. Biotechnol. Bioeng. **41:**263–272.
20. **Favre-Bulle, O., and B. Witholt.** 1992. Biooxidation of *n*-octane by a recombinant *Escherichia coli* in a two-liquid-phase system: effect of medium components on cell growth and alkane oxidation activity. Enzyme Microb. Technol. **14:**931–937.
21. **Fischer, E., N. Zamboni, and U. Sauer.** 2004. High-throughput metabolic flux analysis based on gas chromatography-mass spectrometry derived ^{13}C constraints. Anal. Biochem. **325:**308–316.
22. **Georgellis, D., O. Kwon, and E. C. C. Lin.** 2001. Quinones as the redox signal for the Arc two-component system of bacteria. Science **292:**2314–2316.
23. **Gonzalez-Lergier, J., L. J. Broadbelt, and V. Hatzimanikatis.** 2006. Analysis of the maximum theoretical yield for the synthesis of erythromycin precursors in *Escherichia coli*. Biotechnol. Bioeng. **95:**638–644.
24. **Haddadin, F. T., and S. W. Harcum.** 2005. Transcriptome profiles for high-cell-density recombinant and wild-type *Escherichia coli*. Biotechnol. Bioeng. **90:**127–153.
25. **Hewitt, C. J., G. Nebe-Von Caron, B. Axelsson, C. M. McFarlane, and A. W. Nienow.** 2000. Studies related to the scale-up of high-cell-density *E. coli* fed-batch fermentations using multiparameter flow cytometry: effect of a changing microenvironment with respect to glucose and dissolved oxygen concentration. Biotechnol. Bioeng. **70:**381–390.
26. **Hofstetter, K., J. Lutz, I. Lang, B. Witholt, and A. Schmid.** 2004. Coupling of biocatalytic asymmetric epoxidation with NADH regeneration in organic-aqueous emulsions. Angew. Chem. **43:**2163–2166.
27. **Hüsken, L. E., M. C. Dalm, J. Tramper, J. Wery, J. A. de Bont, and R. Beeftink.** 2001. Integrated bioproduction and extraction of 3-methylcatechol. J. Biotechnol. **88:**11–19.
28. **Jeong, J. Y., Y. J. Kim, N. W. Cho, D. W. Shin, T. W. Nam, S. Ryu, and Y. J. Seok.** 2004. Expression of *ptsG* encoding the major glucose transporter is regulated by ArcA in *Escherichia coli*. J. Biol. Chem. **279:**38513–38518.
29. **Jovanovic, G., L. J. Lloyd, M. P. H. Stumpf, A. J. Mayhew, and M. Buck.** 2006. Induction and function of the phage shock protein extracytoplasmic stress response in *Escherichia coli*. J. Biol. Chem. **281:**21147–21161.
30. **Kantz, A., F. Chin, N. Nallamothu, T. Nguyen, and G. T. Gassner.** 2005. Mechanism of flavin transfer and oxygen activation by the two-component flavoenzyme styrene monooxygenase. Arch. Biochem. Biophys. **442:**102–116.
31. **Kayser, A., J. Weber, V. Hecht, and U. Rinas.** 2005. Metabolic flux analysis of *Escherichia coli* in glucose-limited continuous culture. I. Growth-rate-dependent metabolic efficiency at steady state. Microbiology **151:**693–706.
32. **Kiener, A.** 1992. Enzymatic oxidation of methyl groups on aromatic heterocycles: a versatile method for the preparation of heteroaromatic carboxylic acids. Angew. Chem. **31:**774–775.
33. **Kobayashi, H., M. Yamamoto, and R. Aono.** 1998. Appearance of a stress-response protein, phage-shock protein A, in *Escherichia coli* exposed to hydrophobic organic solvents. Microbiology **144:**353–359.
34. **Laane, C., S. Boeren, K. Vos, and C. Veeger.** 1987. Rules for optimization of biocatalysis in organic solvents. Biotechnol. Bioeng. **30:**81–87.
35. **Li, Z., J. B. van Beilen, W. A. Duetz, A. Schmid, A. de Raadt, H. Griengl, and B. Witholt.** 2002. Oxidative biotransformations using oxygenases. Curr. Opin. Chem. Biol. **6:**136–144.
36. **Liu, X. Q., and P. De Wulf.** 2004. Probing the ArcA-P modulon of *Escherichia coli* by whole genome transcriptional analysis and sequence recognition profiling. J. Biol. Chem. **279:**12588–12597.
37. **Looser, V., F. Hammes, M. Keller, M. Berney, K. Kovar, and T. Egli.** 2005. Flow-cytometric detection of changes in the physiological state of *E. coli* expressing a heterologous membrane protein during carbon-limited fedbatch cultivation. Biotechnol. Bioeng. **92:**69–78.
38. **Lye, G. J., and J. M. Woodley.** 1999. Application of *in situ* product-removal techniques to biocatalytic processes. Trends Biotechnol. **17:**395–402.
39. **Lynch, A. S., and E. C. C. Lin.** 1996. Responses to molecular oxygen, p. 1526–1538. *In* F. C. Neidhardt, R. Curtiss III, J. L. Ingraham, E. C. C. Lin, K. B. Low, B. Magasanik, W. S. Reznikoff, M. Riley, M. Schaechter, and H. E. Umbarger (ed.), *Escherichia coli* and *Salmonella*: cellular and molecular biology, 2nd ed. ASM Press, Washington, DC.
40. **Makart, S., M. Heinemann, and S. Panke.** 2007. Characterization of the AlkS/P_{alkB}-expression system as an efficient tool for the production of recombinant proteins in *Escherichia coli* fed-batch fermentations. Biotechnol. Bioeng. **96:**326–336.
41. **Massey, V.** 1994. Activation of molecular oxygen by flavins and flavoproteins. J. Biol. Chem. **269:**22459–22462.
42. **Messing, J.** 1979. A multipurpose cloning system based on single-stranded DNA bacteriophage M13. Recomb. DNA Technol. Bull. **2:**43–49.
43. **Miller, J. H.** 1972. Experiments in molecular genetics. Cold Spring Harbor Laboratory, Cold Spring Harbor, NY.
44. **Nanchen, A., A. Schicker, and U. Sauer.** 2006. Nonlinear dependency of intracellular fluxes on growth rate in miniaturized continuous cultures of *Escherichia coli*. Appl. Environ. Microbiol. **72:**1164–1172.
45. **Novak, M., T. Pfeiffer, R. E. Lenski, U. Sauer, and S. Bonhoeffer.** 2006. Experimental tests for an evolutionary trade-off between growth rate and yield in *E. coli*. Am. Nat. **168:**242–251.
46. **Onyeaka, H., A. W. Nienow, and C. J. Hewitt.** 2003. Further studies related to the scale-up of high cell density *Escherichia coli* fed-batch fermentations: the additional effect of a changing microenvironment when using aqueous ammonia to control pH. Biotechnol. Bioeng. **84:**474–484.
47. **Otto, K., K. Hofstetter, M. Rothlisberger, B. Witholt, and A. Schmid.** 2004. Biochemical characterization of StyAB from *Pseudomonas* sp. strain VLB120 as a two-component flavin-diffusible monooxygenase. J. Bacteriol. **186:**5292–5302.
48. **Panke, S., V. de Lorenzo, A. Kaiser, B. Witholt, and M. G. Wubbolts.** 1999. Engineering of a stable whole-cell biocatalyst capable of (*S*)-styrene oxide

formation for continuous two-liquid-phase applications. Appl. Environ. Microbiol. **65:**5619–5623.
49. **Panke, S., M. Held, M. G. Wubbolts, B. Witholt, and A. Schmid.** 2002. Pilot-scale production of (*S*)-styrene oxide from styrene by recombinant *Escherichia coli* synthesizing styrene monooxygenase. Biotechnol. Bioeng. **80:**33–41.
50. **Panke, S., B. Witholt, A. Schmid, and M. G. Wubbolts.** 1998. Towards a biocatalyst for (*S*)-styrene oxide production: characterization of the styrene degradation pathway of *Pseudomonas* sp. strain VLB120. Appl. Environ. Microbiol. **64:**2032–2043.
51. **Panke, S., M. G. Wubbolts, A. Schmid, and B. Witholt.** 2000. Production of enantiopure styrene oxide by recombinant *Escherichia coli* synthesizing a two-component styrene monooxygenase. Biotechnol. Bioeng. **69:**91–100.
52. **Park, M. S., J. W. Bae, J. H. Han, E. Y. Lee, S. G. Lee, and S. Park.** 2006. Characterization of styrene catabolic genes of *Pseudomonas putida* SN1 and construction of a recombinant *Escherichia coli* containing styrene monooxygenase gene for the production of (*S*)-styrene oxide. J. Microbiol. Biotechnol. **16:**1032–1040.
53. **Park, J. B.** 2007. Oxygenase-based whole-cell biocatalysis in organic synthesis. J. Microbiol. Biotechnol. **17:**379–392.
54. **Park, J. B., B. Bühler, T. Habicher, B. Hauer, S. Panke, B. Witholt, and A. Schmid.** 2006. The efficiency of recombinant *Escherichia coli* as biocatalyst for stereospecific epoxidation. Biotechnol. Bioeng. **95:**501–512.
55. **Park, J. B., B. Bühler, S. Panke, B. Witholt, and A. Schmid.** 2007. Carbon metabolism and product inhibition determine the epoxidation efficiency of solvent tolerant *Pseudomonas* sp. strain VLB120ΔC. Biotechnol. Bioeng. **98:**1219–1229.
56. **Perrenoud, A., and U. Sauer.** 2005. Impact of global transcriptional regulation by ArcA, ArcB, Cra, Crp, Cya, Fnr, and Mlc on glucose catabolism in *Escherichia coli*. J. Bacteriol. **187:**3171–3179.
57. **Pfeiffer, T., S. Schuster, and S. Bonhoeffer.** 2001. Cooperation and competition in the evolution of ATP-producing pathways. Science **292:**504–507.
58. **Phumathon, P., and G. M. Stephens.** 1999. Production of toluene *cis*-glycol using recombinant *Escherichia coli* strains in glucose-limited fed batch culture. Enzyme Microb. Technol. **25:**810–819.
59. **Russell, J. B., and G. M. Cook.** 1995. Energetics of bacterial growth: balance of anabolic and catabolic reactions. Microbiol. Rev. **59:**48–62.
60. **Sauer, U., F. Canonaco, S. Heri, A. Perrenoud, and E. Fischer.** 2004. The soluble and membrane-bound transhydrogenases UdhA and PntAB have divergent functions in NADPH metabolism of *Escherichia coli*. J. Biol. Chem. **279:**6613–6619.
61. **Schügerl, K., and J. Hubbuch.** 2005. Integrated bioprocesses. Curr. Opin. Microbiol. **8:**294–300.
62. **Schweder, T., E. Krüger, B. Xu, B. Jürgen, G. Blomsten, S. O. Enfors, and M. Hecker.** 1999. Monitoring of genes that respond to process-related stress in large-scale bioprocesses. Biotechnol. Bioeng. **65:**151–159.
63. **Schweder, T., H. Y. Lin, B. Jürgen, A. Breitenstein, S. Riemschneider, V. Khalameyzer, A. Gupta, K. Büttner, and P. Neubauer.** 2002. Role of the general stress response during strong overexpression of a heterologous gene in *Escherichia coli*. Appl. Microbiol. Biotechnol. **58:**330–337.
64. **Sikkema, J., J. A. de Bont, and B. Poolman.** 1995. Mechanisms of membrane toxicity of hydrocarbons. Microbiol. Rev. **59:**201–222.
65. **Staijen, I. E., R. Marcionelli, and B. Witholt.** 1999. The $P_{alkBFGHJKL}$ promoter is under carbon catabolite repression control in *Pseudomonas oleovorans* but not in *Escherichia coli* alk^+ recombinants. J. Bacteriol. **181:**1610–1616.
66. **Stark, D., and U. von Stockar.** 2003. In situ product removal (ISPR) in whole cell biotechnology during the last twenty years. Adv. Biochem. Eng. Biotechnol. **80:**149–175.
67. **Straathof, A. J., S. Panke, and A. Schmid.** 2002. The production of fine chemicals by biotransformations. Curr. Opin. Biotechnol. **13:**548–556.
68. **van Beilen, J. B., W. A. Duetz, A. Schmid, and B. Witholt.** 2003. Practical issues in the application of oxygenases. Trends Biotechnol. **21:**170–177.
69. **Varma, A., and B. O. Palsson.** 1994. Stoichiometric flux balance models quantitatively predict growth and metabolic by-product secretion in wild-type *Escherichia coli* W3110. Appl. Environ. Microbiol. **60:**3724–3731.
70. **Veit, A., T. Polen, and V. F. Wendisch.** 2007. Global gene expression analysis of glucose overflow metabolism in *Escherichia coli* and reduction of aerobic acetate formation. Appl. Microbiol. Biotechnol. **74:**406–421.
71. **Vemuri, G. N., E. Altman, D. P. Sangurdekar, A. B. Khodursky, and M. A. Eiteman.** 2006. Overflow metabolism in *Escherichia coli* during steady-state growth: transcriptional regulation and effect of the redox ratio. Appl. Environ. Microbiol. **72:**3653–3661.
72. **Vemuri, G. N., M. A. Eiteman, and E. Altman.** 2002. Effects of growth mode and pyruvate carboxylase on succinic acid production by metabolically engineered strains of *Escherichia coli*. Appl. Environ. Microbiol. **68:**1715–1727.
73. **Vemuri, G. N., M. A. Eiteman, and E. Altman.** 2006. Increased recombinant protein production in *Escherichia coli* strains with overexpressed water-forming NADH oxidase and a deleted ArcA regulatory protein. Biotechnol. Bioeng. **94:**538–542.
74. **Witholt, B., M.-J. de Smet, J. Kingma, J. B. van Beilen, R. G. Lageveen, and G. Eggink.** 1990. Bioconversions of aliphatic compounds by *Pseudomonas oleovorans* in multiphase bioreactors: background and economic potential. Trends Biotechnol. **8:**46–52.
75. **Wubbolts, M. G., O. FavreBulle, and B. Witholt.** 1996. Biosynthesis of synthons in two-liquid-phase media. Biotechnol. Bioeng. **52:**301–308.